Hindawi
Advances in Materials Science and Engineering
Volume 2021, Article ID 1241797, 17 pages
https://doi.org/10.1155/2021/1241797

Research Article

Experimental and Statistical Investigation of Machinability of AISI D2 Steel Using Electroerosion Machining Method in Different Machining Parameters

Engin Nas,[1] **Onur Özbek**,[2] **Furgan Bayraktar**,[3] **and Fuat Kara**[4]

[1]*Düzce University, Dr. Engin PAK Cumayeri Vocational School, Düzce, Turkey*
[2]*Düzce University, Gümüşova Vocational School, Düzce, Turkey*
[3]*Manufacturing Engineering, Düzce University, Düzce, Turkey*
[4]*Mechanical Engineering, Düzce University, Düzce, Turkey*

Correspondence should be addressed to Engin Nas; enginnas@duzce.edu.tr

Received 5 August 2021; Revised 13 September 2021; Accepted 19 September 2021; Published 22 October 2021

Academic Editor: Abílio De Jesus

This study investigated the effects of machining parameters on the experimental and statistical results using the electric discharge method in the machining of AISI D2 cold work tool steel. The design of the experiment was established using the Taguchi L_{18} method. The effect of the experiment parameters on the performance characteristics was analyzed by analysis of variance (ANOVA). As a result of the study, it was determined that increasing amperage and pulse time affected the surface roughness and hole diameter on the surface of the material. The lowest values for surface roughness, machining time, hole diameter, and crater diameter were determined as 2.085 μm, 47 minutes, 12.010 mm, and 81.007 μm, respectively. The highest wear amount was obtained as 0.604 grams with the processed parameters in the ninth experiment. When the signal-to-noise ratios were examined, the optimum combinations of the control factors for surface roughness, hole diameter, crater diameter, wear amount, wear rate, and processing time were determined as $A_1B_1C_3$, $A_1B_1C_3$, $A_1B_1C_3$, $A_1B_3C_1$, $A_2B_1C_1$, and $A_1B_3C_3$, respectively. According to the ANOVA results, the most important parameters affecting the test results for surface roughness, hole diameter, crater diameter, wear amount, material wear loss, and processing time were determined as amperage (49.34%), time-on (59.38%), amperage (55.65%), time-on (56.92%), amperage (51.42%), and amperage (78.02%), respectively. When the gray relational degree was calculated for the maximum and minimum values, the ideal factors for all output results were found to be the parameters applied in the third experiment.

1. Introduction

The importance of steel material selection in mold production is great. Rather than considering the plastic properties of the raw material to be used, such as hardness and corrosion resistance, in the selection of mold steels, resistance to chemical interaction, surface hardening, and machinability properties should be examined. In addition, parameters such as the design dimensions of the mold, surface polishability, and weldability should be taken into account. Increased mold sizes require higher toughness. Therefore, the heat treatments to be applied may cause deformation problems (distortion, cracking, etc.) during hardening. For these reasons, in the industry, it is advantageous to have prehardened mold steels available [1, 2].

As one of the advanced manufacturing methods, electric discharge machining (EDM) is frequently used in addition to traditional manufacturing techniques in the processing of molded materials. Electric discharge machining is an unusual manufacturing method used for the processing of hard and geometrically complex materials. Although EDM, also known as electroerosion machining, utilizes electrical energy, the material removal process is in the category of thermal processing methods, since it is carried out with thermal energy. The machining performance in EDM has no effect on the stiffness, toughness, and strength of the material

to be machined. The melting temperature and thermal conductivity of the material to be processed are effective in the processing performance. With EDM, chip removal is achieved by melting and evaporating the workpiece. In this technology, electrical sparks are used for material abrasion, so there are no mechanical stresses or tipping and vibration problems during processing as the electrode and workpiece do not touch each other. These EDM features provide an indispensable technology, especially in mold production [3–6].

Many innovations have occurred in the industry with the technological developments. In the manufacturing sector, optimization methods have been developed to determine the effect values of the parameters used during the processing of the product [7]. In the case of more than one test parameter, factorial design is used to test all combinations of levels of each test parameter. In other words, the factorial test design is a combination of multiple levels in experiments in which there are at least two or more test parameters and at least two or more levels of these parameters [8]. When combined with statistical methods, the full factorial experimental design provides great convenience to researchers during the analysis process. Analysis of variance (ANOVA) and regression analysis are used in the analysis of full factorial experiments. The ANOVA reveals which test parameters are statistically important in the process [9]. Regression analysis is used to determine the existence of a clear mathematical relationship between cause (independent input variables) and result (dependent output variables) [10]. By applying these methods, it is possible to calculate the effect of a factor on the experiment and to determine the source of the differences without making a change in the order of the operations [11, 12].

Taguchi test design is a successful method used for solving optimization problems by increasing the processing performance with a minimum number of tests and low cost. Due to the vertical indices developed by Taguchi, the number of experiments is significantly reduced, thus preventing the loss of time and money. The advantage of the Taguchi method is that it can predict the result. The Taguchi method not only ensures that the solution is achieved with the least number of experiments but also supports the development of high-quality processes and products in every respect. It shows minimum sensitivity against process or product production conditions or against uncontrollable factors. Due to the loss function, the Taguchi method develops a new concept of quality cost by minimizing the total loss caused by the product [13, 14].

The literature studies on the machinability of AISI D2 cold work tool steel in EDM have been examined and summarized. Matin et al. examined the wear loss of electrode material and of DIN 1.2379 cold work tool steel using different machining parameters and electrode shapes (triangular, square, and circular) on the EDM machine. As a result of the study, it was determined that the maximum material wear and tool wear amount was with 42 amperes at 50 μs pulse time-on and the highest tool wear amount was with 42 amperes at 20 μs pulse time-on [15]. In his experimental work, Gov investigated the drilling of AISI D2 cold work tool steel on an EDM machine. The drilling parameters were determined as pulse time, waiting time, amperage, dielectric pressure, single-hole electrode, and different temperatures of dielectric fluid. The effect of the experiments carried out at different dielectric water temperatures on the surface roughness, white layer thickness, taper, material wear, and tool wear amount was examined. As a result of the study, it was determined that the surface roughness, hole taper, and white layer thickness decreased, and material wear loss and tool wear loss increased at temperatures below zero [16]. In another study, Gov carried out the drilling process on AISI D2 mold steel via the EDM using different electrode materials. He investigated the effects of electrodes with different channels (single channel and multiple channels) on electroerosion drilling performance by keeping the processing parameters constant. As a result of the study, it was determined that the processing speed of the single-channel brass electrode was higher and electrode wear was lower compared to multichannel brass and copper electrodes. In addition, surface roughness and white layer thickness values were determined to be better than with other electrodes when single-channel brass electrodes were used [17]. In their study, Anitha et al. reported the results obtained by processing AISI D2 die steel on an EDM machine with processing parameters determined as discharge current, pulse time, waiting time, and voltage, with three different values for each factor. As a result of the study, in order to find the most suitable conditions for the regression model developed with response surface methodology (RSM) for minimum surface roughness, the results were analyzed again with genetic algorithm (GA) and the formula to minimize the processing time was determined [18]. In his study, Ali investigated the machining of AISI D2 cold work tool steel on an EDM machine with different processing parameters (amperage and time-on) using a copper electrode. The study examined surface roughness, workpiece machining speed, electrode wear rate, and relative wear values of the treated surfaces. As a result, it was determined that the increase of discharge current and pulse duration adversely affected the surface roughness and electrode wear rate and positively affected the workpiece machining speed [19].

This study examined AISI D2 cold work tool steel machined on an EDM machine using different machining parameters and electrodes. The difference from other studies is the measurement of holes and craters formed on the processed surfaces. Surface roughness values, electrode wear, material wear losses, hole diameters, and crater diameters were then investigated both experimentally and statistically. For the statistical analysis, the data sheet was prepared using the Taguchi L_{18} experimental design method. Parameters used in the experiments, taking into account the literature research, were determined as three different machining times, three different pulse times, and two different discharge current values along with a constant cutting depth. After the experiments, surface roughness values, crater diameters, hole diameters formed by the electrode, material wear loss, and processing times were measured. The results were investigated experimentally and statistically using

ANOVA, regression, and gray relational degree analyses in order to determine the ideal parameters.

2. Materials and Methods

2.1. Electrical Discharge Machining (EDM). In the present study, the King ZNC-K-3200 EDM machine was used. After each experiment was carried out, the machined surface was cleaned of the electrode material using a universal turning lathe. Images of the material before and during processing are given in Figure 1.

Graphite was selected as the electrode material because of its excellent thermal and electrical conductivity and high temperature resistance [20]. The graphite electrode used had a density of 2 g cm^{-3}, a length of 100 mm, and a diameter of 12 mm.

2.2. Workpiece Material. The AISI D2 cold work tool steel was used in the experiments. This tool steel is generally preferred for use in the manufacture of bolt rollers, cold forming molds, precision cutting molds for sheet metal of up to 6 mm in thickness, cold punches, deep drawing molds, high abrasive plastic molds, breaking knives, cold rolling reels, chip knives, fracture-exposed sections, scissor blades, deburring molds, and woodworking tools [21]. The chemical composition of the steel material used in the study is given in Table 1.

2.3. Machining Parameters. In the experimental study, the test parameters used in the processing of AISI D2 steel in the EDM machine were determined as pulse duration (time-on), discharge current (amperes), constant waiting time (time-off), and constant cutting depth. The experimental design was determined according to Taguchi L_{18}, and the factors and levels are shown in Table 2.

In order to determine the parameters shown in Table 2, preliminary experiments were performed after reviewing the relevant literature studies. Consequently, it was determined that, during the discharge of the current to the material surface, molten particles adhered to the electrode material when it came in contact with the pressurized dielectric fluid (Figure 2). As a solution to this problem, the EDM reservoir was filled with a certain quantity of the dielectric fluid (5–10 mm) and set to be spread over the workpiece surface, and the experiments were carried out without spraying the fluid. Afterwards, it was observed that the molten particles did not adhere to the surface of the electrode material.

2.4. Average Surface Roughness, Weight Loss, Crater, and Hole Diameter Measurements. The Mahr MarSurf PS 10 Portable surface roughness tester was used to measure surface roughness values. According to ISO 4287 standard, the surface roughness measurements were performed at room temperature and conducted in three repetitions [2]. Surface roughness values are measured at three different locations from the machined surfaces and their average determines the roughness (Ra) values. The weight loss measurements of

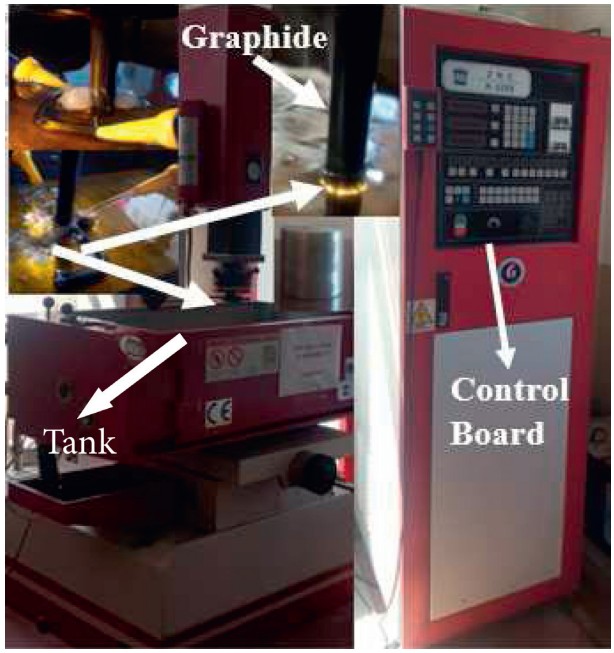

Figure 1: Electrical discharge processing machine used in the experimental study.

Table 1: Chemical composition (%) of the AISI D2 (raw material) cold work tool steel used in the study.

C	Cr	Mo	V
1.55	12.0	0.8	0.9

Table 2: Taguchi L_{18} test parameters and levels used in the experimental study.

Factors	Level 1	Level 2	Level 3
Time on (μs)–(A)	20	40	60
Time off (μs)–(B)	200	400	600
Ampere (A)–(C)	2	4	—
Cutting depth (mm)		0.5	

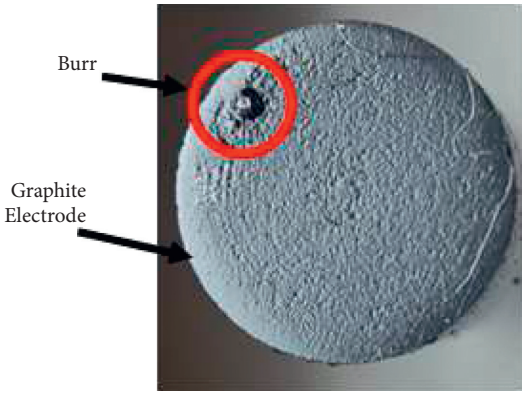

Figure 2: Molten material adhered to the electrode surface during the pretests.

the test samples were made using the RADWAG precision scale (0.001 g accuracy). Hole and crater diameter measurements and images were determined using the Dino-Lite optical microscope.

3. Results and Discussion

3.1. Input Parameters and Output Values. After the literature review, experiments were carried out with the selected processing parameters. The measurements were performed in three repetitions from different locations and the average was taken (Table 3).

3.2. Processing Time. Figure 3 shows a graphical representation of the processing times obtained from the experiments performed on the EDM machine. After examining the graphs, it was determined that, in the experiments carried out with 2 amperes, the maximum processing time was 400 μs pulse time-on and 60 μs time-off and the shortest processing time was 200 μs pulse time-on and 20 μs time-off. In the experiments carried out with 4 amperes, it was determined that the processing time was increased with increasing pulse time-on. The shortest processing time was 200 μs pulse time-on and 20 μs time-off, whereas the maximum processing time was 600 μs pulse time-on and 60 μs time-off. It is reported in the literature that processing time decreases with increasing pulse time-on, while in the experiments carried out at 4 amperes, the opposite trend occurred [19]. This situation could be explained in two ways. The first is that, during the discharge of the current on the material, the molten material adhering to the electrode surface increased the processing time. The second is that the increased pulse duration affected the mechanical properties of the material and made chip removal difficult.

3.3. Wear Amount and Material Removal Rate (MRR). In the experiments performed with EDM, material wear losses per minute were calculated by recording the time from the first arc to the end. The material removal rate (MRR) was calculated from the difference of the weight before and after machining of the workpiece carried out per minute. The formula for calculation of the MRR is given as follows:

$$\text{material removal rate} = \left[\frac{\left(W_i - W_f\right)}{t}\right]. \quad (1)$$

MRR is material removal rate (g/min), W_i is initial weight of workpiece (before machining) (g), W_f is final weight of workpiece (after machining) (g), and t is period of trial (min).

In the experimental study, the values given in Table 3 are shown graphically in Figures 4 and 5. The graphs show that the amount of wear increased with the decrease of the time-off and the lowest amount of wear occurred at 400 μs pulse time-on and 60 μs time-off at 2 amperes.

3.4. Surface Roughness and Crater Diameter. The results obtained (Table 3) for the effects of processing parameters are shown in graphic form in Figure 6, which shows that low values for surface roughness and crater diameter were obtained with low amperage, low pulse duration, and high waiting time.

The lowest surface roughness and crater diameter values were determined at 2 amperes, 200 μs pulse time-on and 60 μs time-off, whereas the highest values were found at 600 μs pulse time-on and 20 μs time-off. It was determined that increased amperage and pulse duration affected the crater diameter and this situation adversely affected the surface roughness [22]. The profilometer images of the experiments with the lowest surface roughness and the highest surface roughness value are shown in Figure 7.

Optical and scanning electron microscope (SEM) images taken of the craters formed on the material surfaces where the minimum and maximum surface roughness values that occurred are shown in Figure 8.

The optical images (Figure 8) show the effect of amperage and pulse duration on the surface of the material. At the low amperage, low time-on, and high time-off, a smooth surface structure was formed, while at high amperage, high time-on, and low time-off, a defective surface was formed. Higher discharge current increases the amount of particles melting and evaporating from the workpiece. This leads to the formation of larger craters on the workpiece surface. The size of the craters causes the surface roughness value to increase. Craters are cavities formed by spherical chips removed from the surface by the effect of each spark during processing. Electroerosion processing is characterized by the use of high local voltages and temperatures, which cause erosion and vaporization of the material. Therefore, in electroerosion machining, that is, EDM, the machined surfaces have a nondirectional profile [19, 23, 24].

3.5. Hole Diameter. The values in Table 3 which are shown graphically in Figure 9 give the effects of the machining parameters on hole diameters in the experiments carried out by EDM. When the graphs are examined, it can be seen that the hole diameter was larger than the electrode diameter with decreasing time-off and increasing of amperage and pulse time-on.

It was determined that the discharge current application of the electrode to the side walls of the hole caused the hole diameter to be greater than that of the electrode and, therefore, in order to obtain a specific hole diameter, the discharge current should be considered [25].

3.6. Taguchi Method. Some experimental design variables cannot be controlled or expressed using traditional methods. However, the Taguchi method achieves this by converting the values of the objective functions to signal/noise (S/N) ratios and measuring the control factor level performance characteristics. The S/N ratio is defined as the desired signal ratio for the undesired random noise value which indicates the quality characteristics of the experimental data.

Signal-to-noise (S/N) analysis for surface roughness, hole diameter, crater diameter, wear amount, wear rate, and processing time were used in the optimization of the control

Table 3: Test parameters and output parameters obtained after processing.

No.	Ampere	Time on (μs)	Time off (μs)	Processing time (min.)	Wear amount (g)	Wear rate (g/min)	Surface roughness (μm)	Hole diameters (mm)	Crater diameter (μm)
1	2	200	20	192	0.421	0.0022	2.363	12.466	85.446
2	2	200	40	346	0.421	0.0012	2.149	12.462	83.790
3	2	200	60	387	0.367	0.0009	2.085	12.432	81.007
4	2	400	20	272	0.434	0.0016	3.394	12.565	104.556
5	2	400	40	422	0.336	0.0008	3.205	12.529	100.209
6	2	400	60	430	0.301	0.0007	3.191	12.039	96.151
7	2	600	20	270	0.547	0.0020	3.548	12.555	107.506
8	2	600	40	306	0.531	0.0017	3.430	12.010	105.901
9	2	600	60	378	0.604	0.0016	3.381	12.522	104.470
10	4	200	20	47	0.418	0.0089	3.659	12.503	109.953
11	4	200	40	67	0.380	0.0057	3.520	12.500	105.348
12	4	200	60	110	0.313	0.0028	3.456	12.464	104.916
13	4	400	20	63	0.395	0.0063	3.920	12.587	124.843
14	4	400	40	102	0.404	0.0040	3.880	12.525	123.893
15	4	400	60	155	0.349	0.0023	3.700	12.505	121.695
16	4	600	20	87	0.483	0.0056	4.714	12.656	143.165
17	4	600	40	138	0.452	0.0033	4.443	12.644	140.170
18	4	600	60	176	0.401	0.0023	4.083	12.551	137.911

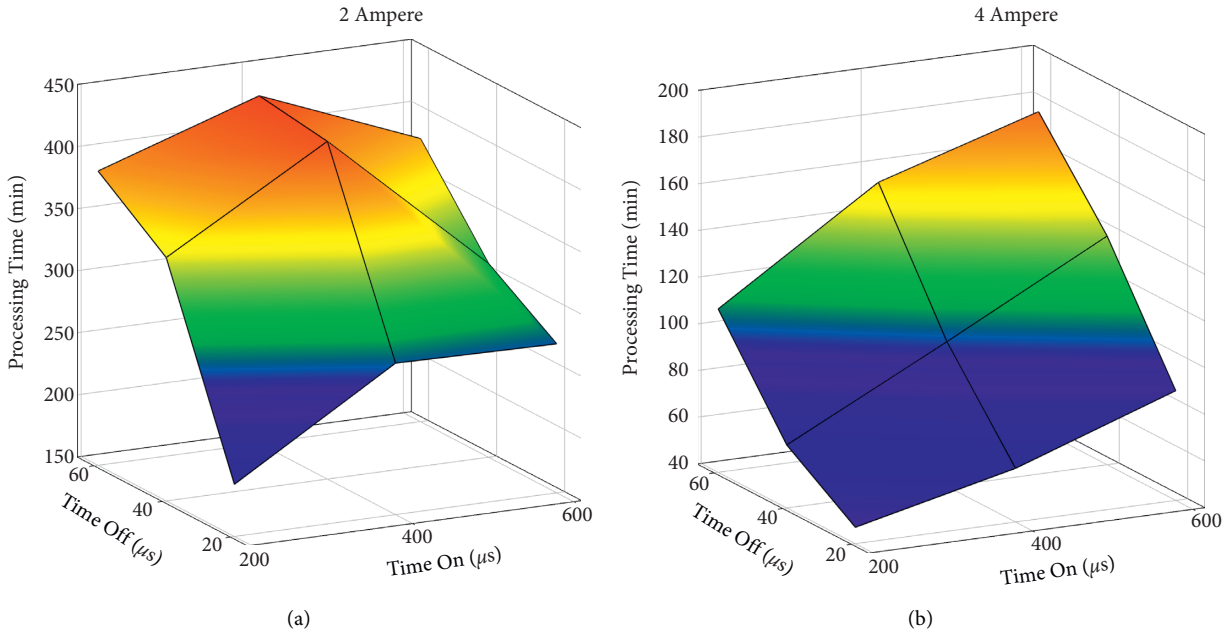

Figure 3: Effect of pulse time-on and time-off on processing time at 2 (a) and 4 (b) amperes.

factors. In the method used for the calculation of S/N ratios, depending on the characteristic type, the objective functions were given as "the smallest is best" (equation (2)) and "the largest is best" (equation (3)) [26].

$$\frac{S}{N} = -10\log\left(\frac{1}{n}\sum_{i=1}^{n} y_i^2\right), \tag{2}$$

$$\frac{S}{N} = -10\log\left(\frac{1}{n}\sum_{i=1}^{n}\frac{1}{y_i^2}\right). \tag{3}$$

The S/N response table obtained for the formation of ideal parameters for surface roughness, hole diameter, crater diameter, wear amount, wear rate and processing time is given in Table 4 and shown graphically in Figure 10. In determining the optimum levels of the control factors, the maximum S/N values in the S/N response table generated by the Taguchi method indicate the ideal level of that control factor [27].

According to the S/N ratios, the ideal levels for surface roughness, hole diameters, crater diameters, wear amount, wear rate, and processing time were determined

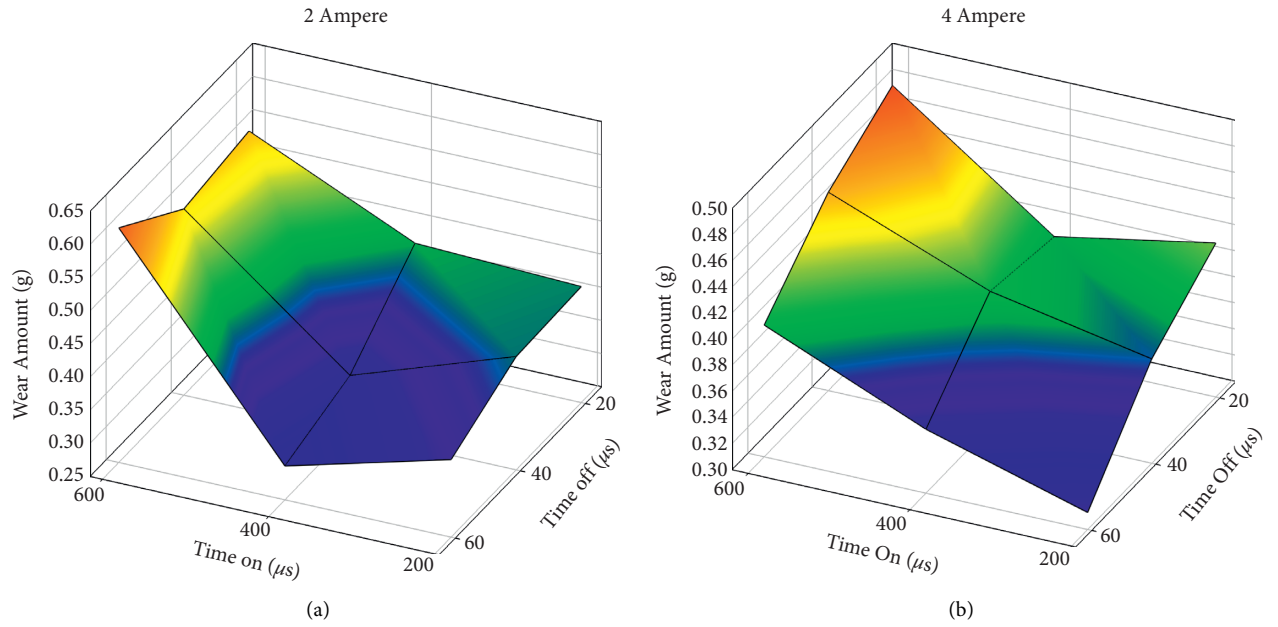

Figure 4: Effect of pulse time-on and time-off on wear amount at 2 (a) and 4 (b) amperes.

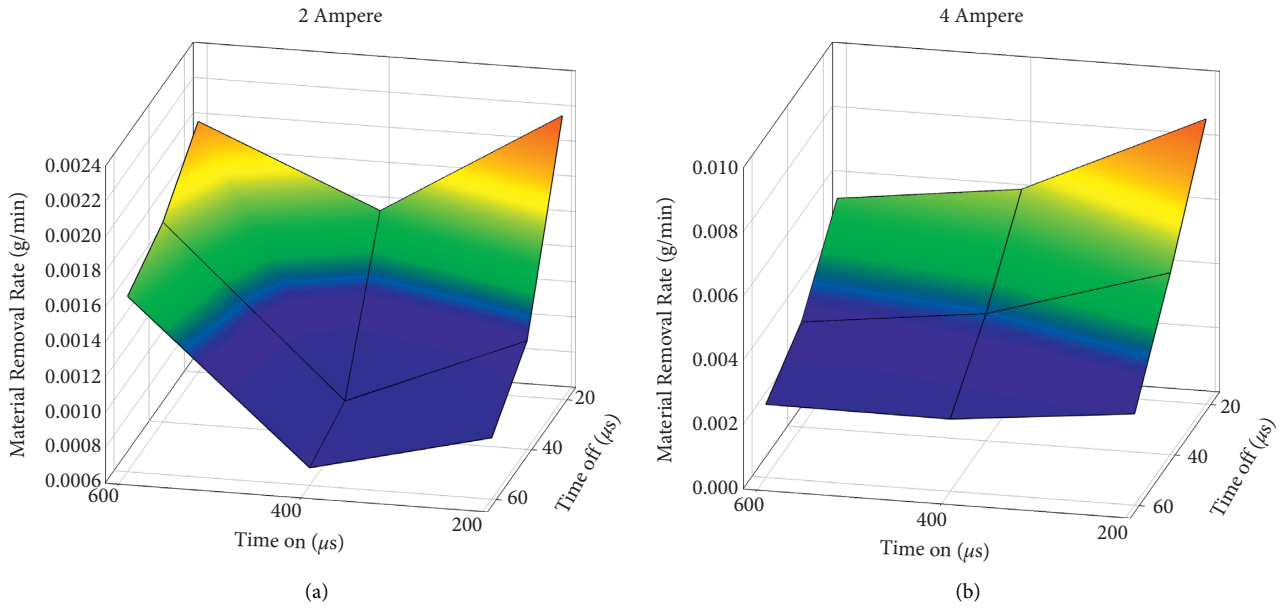

Figure 5: Effect of pulse time-on and time-off on wear rate at 2 (a) and 4 (b) amperes.

as $A_1B_1C_3$, $A_1B_1C_3$, $A_1B_1C_3$, $A_1B_3C_1$, $A_2B_1C_1$, and $A_1B_3C_3$, respectively [28].

3.7. ANOVA. Individual interactions among all experimental design control factors can be determined by the use of the ANOVA statistical method [29]. This study applied ANOVA for the analysis of the effects of pulse duration, waiting time, and discharge current (amperes) on surface roughness, hole and crater diameters, wear amount and rate, and machining time. The levels of significance and confidence for this analysis were determined as 0.05 and 95%, respectively. In order to determine the significance of the control factors, ANOVA compares the *F*-values for each individual control factor [28]. The ANOVA results for the surface roughness, hole diameter, crater diameter, wear amount, wear rate, and processing time are shown in Table 5 as 93.55%, 83.34%, 97.65%, 73.58%, 80.82%, and 92.22%, respectively, which are shown in bold.

According to the ANOVA, the most effective parameters for surface roughness, hole diameter, crater diameter, wear amount, wear rate, and processing time were determined as

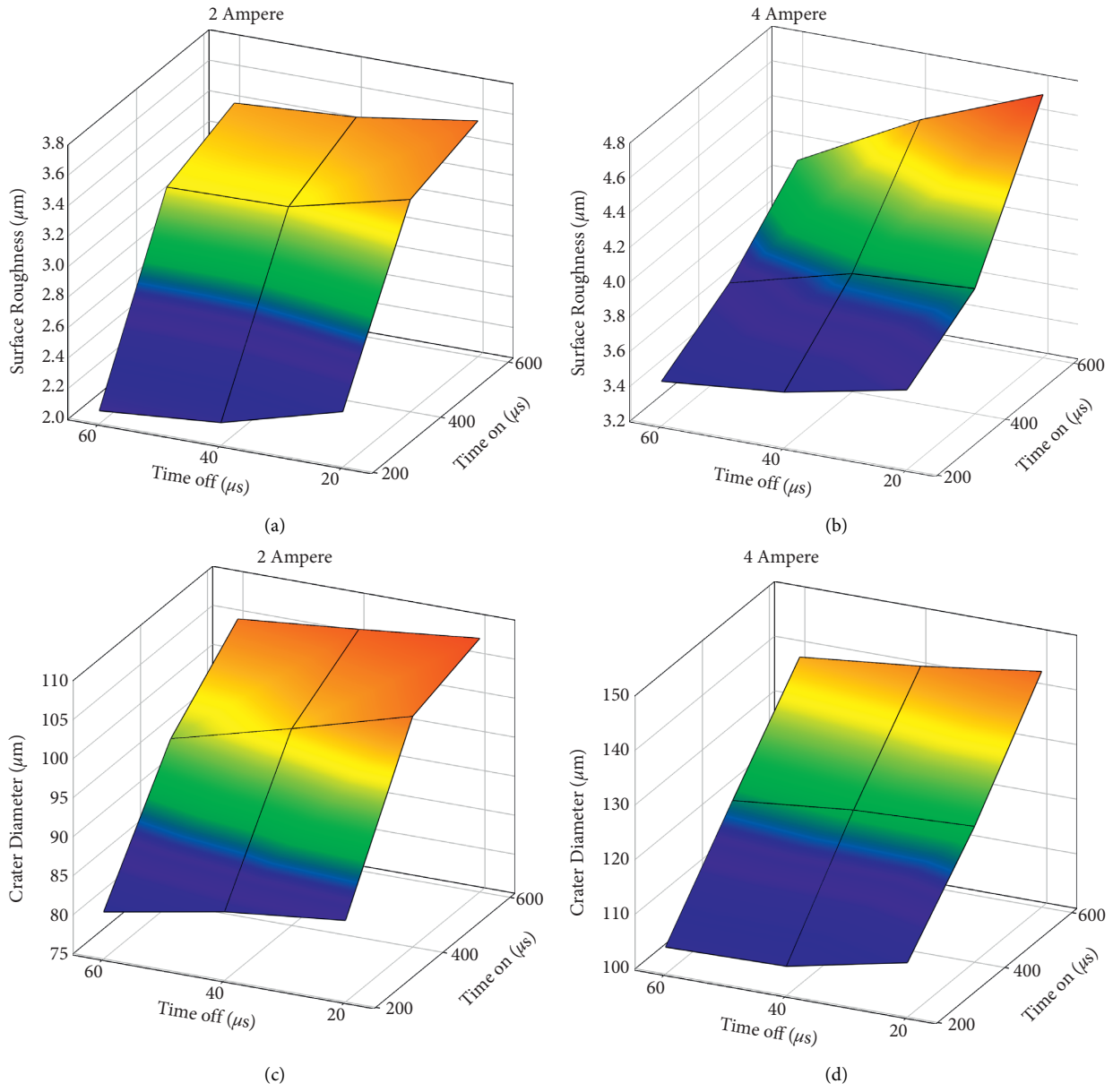

Figure 6: Effect of pulse time-on and time-off on surface roughness and crater diameters at 2 (a, c) and 4 (b, d) amperes.

amperage **(49.34%)**, pulse duration **(59.38%)**, amperage **(55.65%)**, pulse duration **(56.92%)**, amperage **(51.42%),** and amperage **(78.02%)**, respectively.

3.8. Regression Analysis of Surface Roughness, Hole Diameter, Crater Diameter, Wear Amount, Material Removal Rate, and Machining Time. Regression analyses can carry out modeling and analysis for different variables when a relationship exists between a dependent variable and one or a number of independent variables [29, 30]. In this study, the equations for estimation of surface roughness, hole diameter, crater diameter, wear amount, material removal rate, and machining time were calculated using regression analysis. Linear regression model equations are shown in Table 6.

3.9. Estimation of Optimum Surface Roughness, Hole Diameter, Crater Diameter, Wear Amount, Wear Rate, and Processing Time. It was necessary to evaluate whether or not the system had realized the optimization accurately enough. For this purpose, the following equations were used in the specification of the confidence interval (CI) [31, 32] for estimated

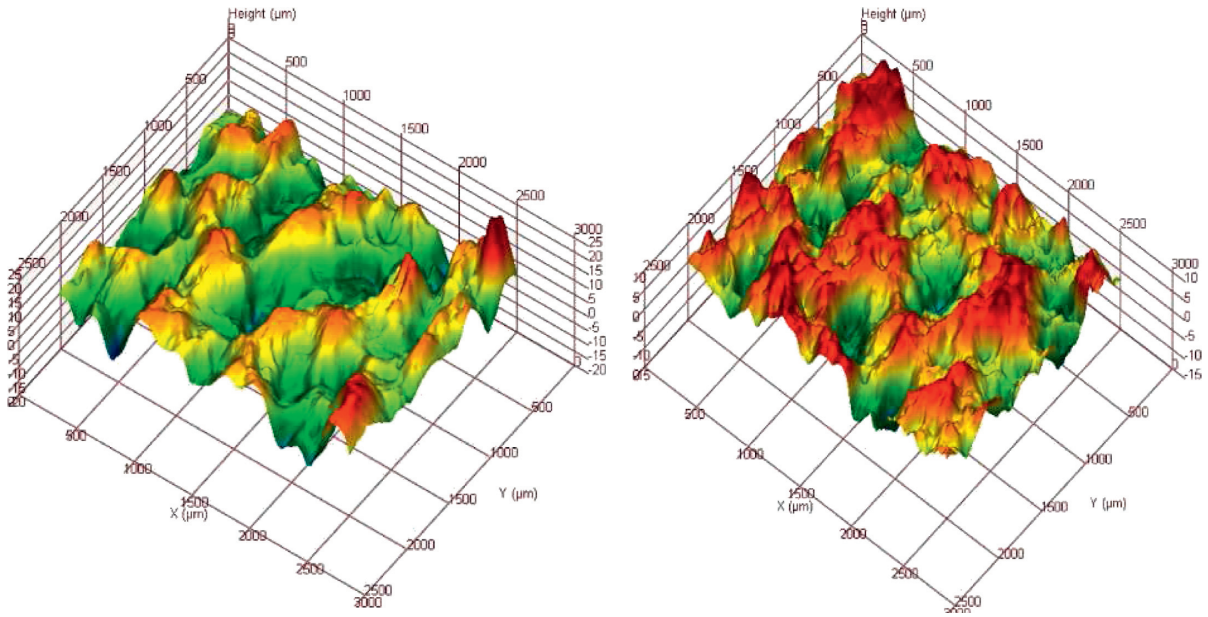

(a) (b)

Figure 7: Optical profilometer images of the surfaces with the lowest (a) and highest (b) surface roughness values.

surface roughness, hole diameter, crater diameter, wear amount, wear rate, and processing time.

Optimal results were obtained using the Taguchi approach. The estimated optimum values were calculated using the six following equations, respectively:

$$\text{surface roughness} = T_{\text{Ra}} + (A_1 - T_{\text{Ra}}) + (B_1 - T_{\text{Ra}}) + (C_3 - T_{\text{Ra}}), \tag{4}$$

$$\text{hole diameter} = T_{\text{HD}} + (A_1 - T_{\text{HD}}) + (B_1 - T_{\text{HD}}) + (C_3 - T_{\text{HD}}), \tag{5}$$

$$\text{crater diameter} = T_{\text{CD}} + (A_1 - T_{\text{CD}}) + (B_1 - T_{\text{CD}}) + (C_3 - T_{\text{CD}}), \tag{6}$$

$$\text{MRR} = T_{\text{MRR}} + (A_2 - T_{\text{MRR}}) + (B_1 - T_{\text{MRR}}) + (C_1 - T_{\text{MRR}}), \tag{7}$$

$$\text{wear amount} = T_{\text{WA}} + (A_1 - T_{\text{WA}}) + (B_3 - T_{\text{WA}}) + (C_1 - T_{\text{WA}}), \tag{8}$$

$$\text{processing time} = T_{\text{PT}} + (A_1 - T_{\text{PT}}) + (B_3 - T_{\text{PT}}) + (C_3 - T_{\text{PT}}). \tag{9}$$

T_{Ra}, T_{HD}, T_{CD}, T_{WA}, T_{MRR}, and T_{PT} state the average of all the values obtained from the experiments. The confidence interval (CI) was obtained by comparing the verification experimental values with the values determined by the estimations. Equations (10) and (11) were used to calculate the CI for the surface roughness, hole and crater diameters, wear amount and rate, and machining time. The values from the estimation were expected to be within the CI range [28]. An explanation of the symbols found in the equations for CI is given in the Abbreviations section.

$$\text{CI} = \sqrt{F_{\alpha;1;f_e} x V_e x \left(\frac{1}{n_{\text{eff}}} + \frac{1}{r}\right)}. \tag{10}$$

n_{eff} formula is as follows:

$$n_{\text{eff}} = \frac{N}{1 + [T_{\text{dof}}]}. \tag{11}$$

The average optimal surface roughness with the CI at 95% was estimated as follows:

$$\begin{aligned}&[\text{TRa, TMRR, THD, TCD, TMRR, TWA and TPT}] - [\text{CI}] < (\text{TRa, TMRR, THD, TCD, TMRR, TWA and TPT})\\ &\text{exp} < [\text{TRa, TMRR, THD, TCD, TMRR, TWA and TPT}] + [\text{CI}].\end{aligned} \tag{12}$$

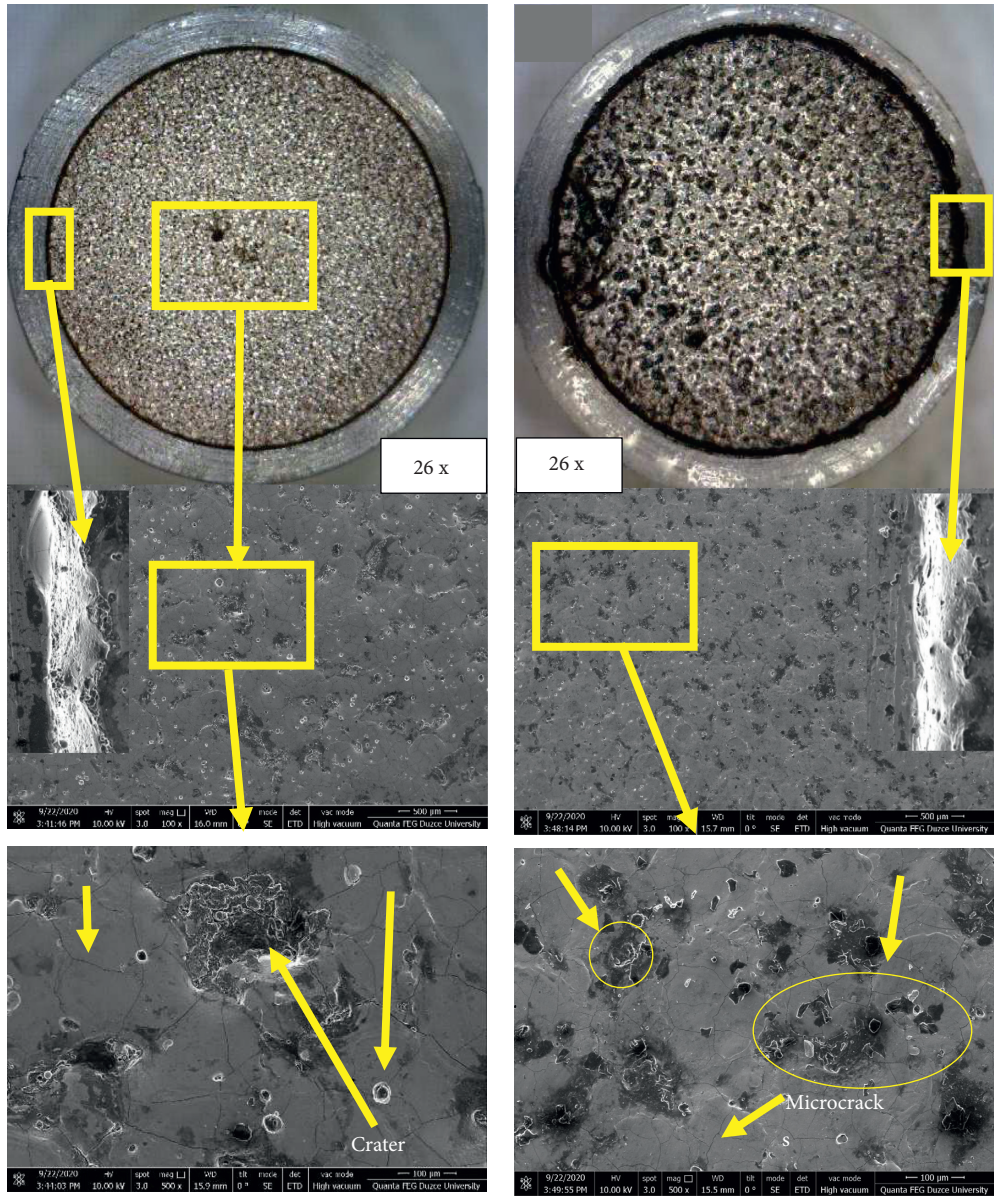

FIGURE 8: Optical and SEM images of the surfaces having the lowest (a) and highest (b) surface roughness values according to the machining parameters.

Quadratic regression analysis was then applied to determine whether the predicted values of the experimental results were within the CI and PI (predicted internally). This test was performed to determine the relationship between the predicted values using the Taguchi optimization method and the experimental results. When the results were evaluated, it was found that the estimated values were within the CI (95%) and PI (95%) limits in the regression analysis (Figure 11).

3.10. Gray Relational Analysis. Since the Taguchi method determines the effects and optimal levels of the control factors by way of a small number of experiments, it is an efficient method which is preferred in experimental studies. However, it is applicable only in single-answer optimization problems. Therefore, the conventional Taguchi method alone cannot optimize a multipurpose optimization problem but is used in combination with gray relational analysis to optimize these kinds of problems. Gray relational analysis is a tool for decision-making and analysis. Gray theory was first put forward in 1982 by Professor Julong Deng. Gray relational analysis is known to be applied in different industrial areas under the headings of gray modeling, gray prediction, and gray decision-making. In gray relationship analysis, black shows that it does not have the information, and white shows that it has the information completely. The gray system shows the level of information between black and white. In the gray system, while some of the information is known, some parts are unknown [33]. In the white system,

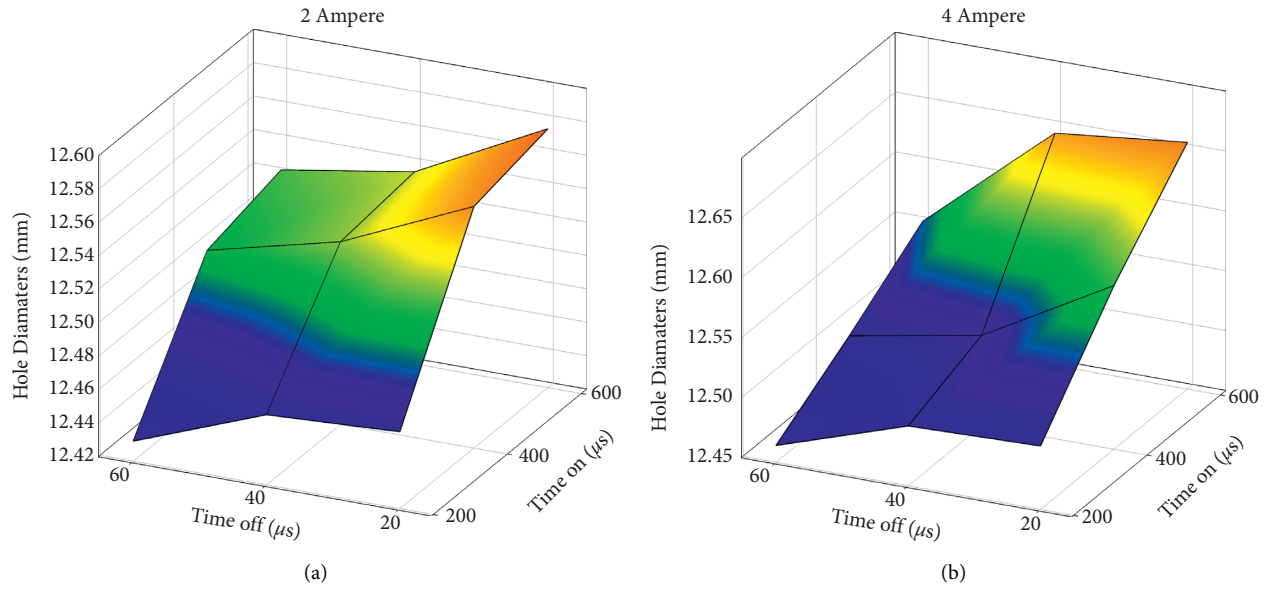

Figure 9: Effect of pulse time-on and time-off on hole diameter at 2 (a) and 4 (b) amperes.

Table 4: Signal/noise values obtained from the experimental study.

Surface roughness (μm)				Hole diameters (mm)				Crater diameters (μm)			
Level	Ampere	Time on (μs)	Time off (μs)	Level	Ampere	Time on (μs)	Time off (μs)	Level	Ampere	Time on (μs)	Time off (μs)
1	−9.288	−8.911	−10.947	1	−21.95	−21.92	−21.98	1	−39.65	−39.49	−40.92
2	−11.846	−10.969	−10.521	2	−21.97	−21.96	−21.96	2	−41.78	−40.93	−40.70
3		−11.821	−10.233	3		−21.99	−21.94	3		−41.72	−40.52
Delta	2.558	2.910	0.715	Delta	0.03	0.08	0.04	Delta	2.13	2.23	0.40
Rank	2	1	3	Rank	3	1	2	Rank	2	1	3
Wear amount (g)				Wear rate (g/min)				Processing times (min.)			
Level	Ampere	Time on (μs)	Time off (μs)	Level	Ampere	Time on (μs)	Time off (μs)	Level	Ampere	Time on (μs)	Time off (μs)
1	−7.334	−8.301	−6.995	1	−57.55	−51.47	−48.86	1	50.22	43.17	41.87
2	−8.034	−8.706	−7.610	2	−47.73	−54.34	−53.03	2	39.69	45.64	45.42
3		−6.046	−8.447	3		−52.11	−56.03	3		46.06	47.59
Delta	0.700	2.660	1.452	Delta	9.82	2.88	7.17	Delta	10.52	2.90	5.72
Rank	3	1	2	Rank	1	3	2	Rank	1	3	2

the interrelationship factors in the system are definite, whereas, in the gray system, the interrelationship factors in the system are uncertain [34]. The calculation steps of the gray relational analysis method are as follows.

Step 1. Ranking of the reference values (surface roughness, hole diameter, crater diameter, wear amount, wear rate, and processing time) using the following equation:

$$x_0 = \left(x_0(1),\ x_0(2), x_0(3), \ldots x_0(n)\right). \tag{13}$$

Step 2. Normalization of the data obtained from the test results.

Linear data processing is among the common methods applied for normalization. For example, "the lowest is best" should be preferred in the normalization of surface roughness. In linear normalization, the points that take small values in surface roughness take values close to "1." Points that receive large values will take values close to "0." In the case of "the highest is best," normalization is as in the following equation:

$$x_i(k) = \frac{x_i^0(k) - \min x_i^0(k)}{\max x_i^0(k) - \min x_i^0(k)}. \tag{14}$$

$x_i^0(k)$ in the i series k is the ranked as the original value; $x_i\ (k)$ after normalization of i series k is the next value; $\min x_i^0(k)$ is the minimum value in the i series; $\max x_i^0(k)$ is the maximum value in the i series.

In the case of "the lowest is best," normalization is as in the following equation [35]:

$$x_i(k) = \frac{\max x_i^0(k) - x_i^0(k)}{\max x_i^0(k) - \min x_i^0(k)}. \tag{15}$$

In the case of "the ideal value is best," normalization is as in the following equation:

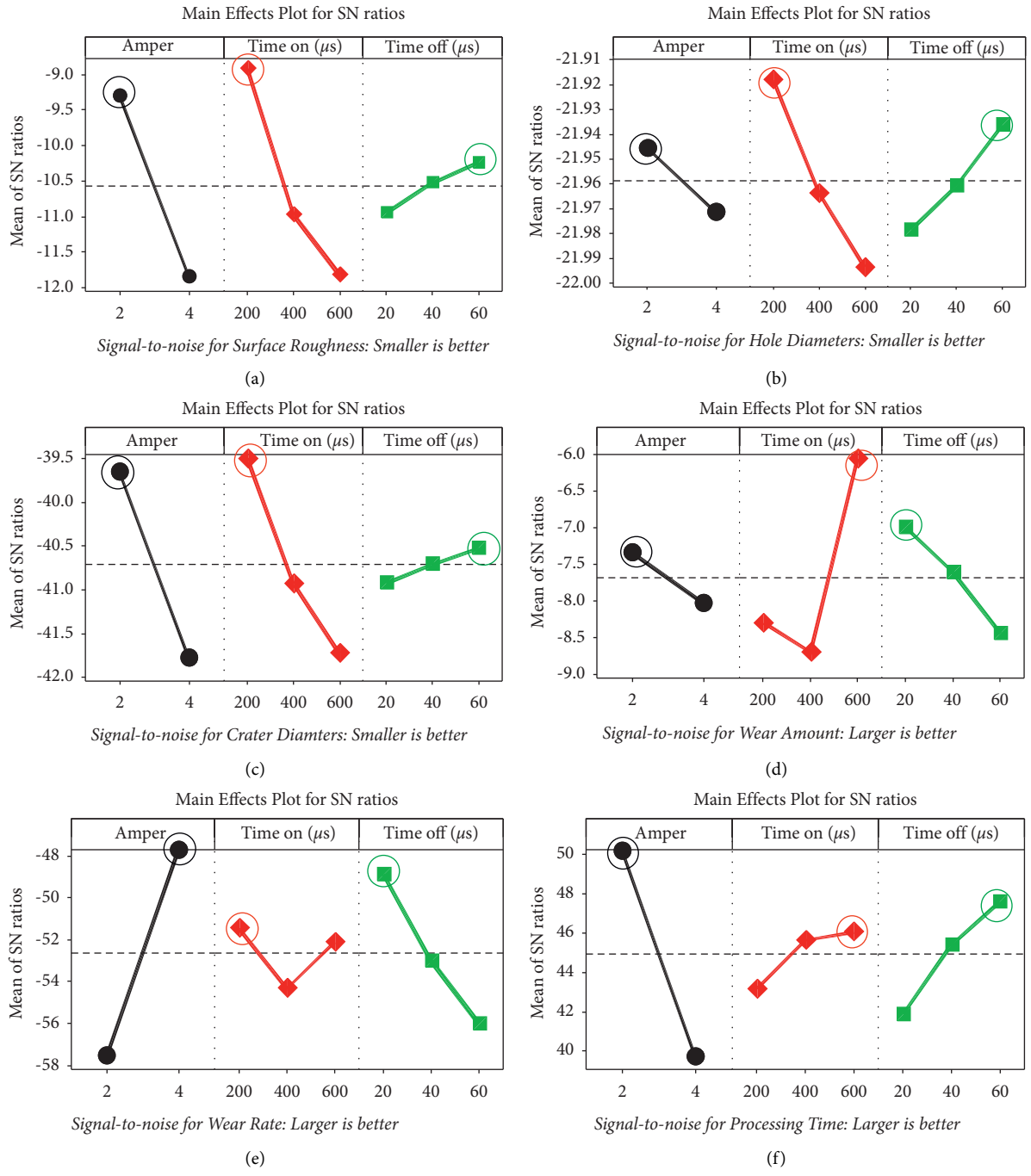

FIGURE 10: Main effect plot for signal/noise analysis values ((a) surface roughness, (b) hole diameter, (c) crater diameter, (d) wear amount, (e) wear rate, and (f) processing time).

$$x_i(k) = 1 - \frac{\left|x_i^0(k) - x^0\right|}{\max x_i^0(k) - x^0}. \tag{16}$$

Here, x_0 represents the desired ideal value.

Step 3. Let the "m" series be compared to the "xi" series, as defined in the following equation:

$$x_i = \left(x^i(1), x^i(2), x^i(3), \ldots\ldots x^i(n)\right), \quad i = 1, 2, \ldots, m. \tag{17}$$

Step 4. Let k, in the series k. n be shown in the order: $e(x_0(k), x_i(k))$. The gray relational coefficient at point k is calculated according to the following four equations:

Table 5: ANOVA results.

Analysis of variance for surface roughness							
Source	DF	Seq. SS	Contribution (%)	Adj. SS	Adj. MS	*F* value	*P* value
Ampere	1	4.1366	49.34	4.1366	4.13665	91.78	0.000001
Time on (μs)	2	3.4632	41.31	3.4632	1.73160	38.42	0.000006
Time off (μs)	2	0.2430	2.90	0.2430	0.12150	2.70	0.107923
Error	12	0.5409	6.45	0.5409	0.04507		
Total	17	8.3837	100.00		**R-sq: 93.55%**		
Analysis of variance for hole diameter							
Source	DF	Seq. SS	Contribution (%)	Adj. SS	Adj. MS	*F* value	*P* value
Ampere	1	0.006385	10.44	0.006385	0.006385	10.75	0.006601
Time on (μs)	2	0.036316	59.38	0.036316	0.018158	30.57	0.000020
Time off (μs)	2	0.011332	18.53	0.011332	0.005666	9.54	0.003316
Error	12	0.007129	11.66	0.007129	0.000594		
Total	17	0.061161	100.00		**R-sq: 88.34%**		
Analysis of variance for crater diameter							
Source	DF	Seq. SS	Contribution (%)	Adj. SS	Adj. MS	*F* value	*P* value
Ampere	1	3276.67	55.65	3276.67	3276.67	283.97	0.000000001
Time on (μs)	2	2401.05	40.78	2401.05	1200.53	104.04	0.000000026
Time off (μs)	2	71.88	1.22	71.88	35.94	3.11	0.081360841
Error	12	138.47	2.35	138.47	11.54		
Total	17	5888.07	100.00		**R-sq: 97.65%**		
Variance analysis for wear amount							
Source	DF	Seq. SS	Contribution (%)	Adj. SS	Adj. MS	*F* value	*P* value
Ampere	1	0.007483	6.75	0.007483	0.007483	3.07	0.105
Time on (μs)	2	0.063100	56.92	0.063100	0.031550	12.93	0.001
Time off (μs)	2	0.010987	9.91	0.010987	0.005493	2.25	0.148
Error	12	0.029288	26.42	0.029288	0.002441		
Total	17	0.110858	100.00		**Rq: 73.58%**		
Variance analysis for wear rate							
Source	DF	Seq. SS	Contribution (%)	Adj. SS	Adj. MS	*F* value	*P* value
Ampere	1	0.000044	51.42	0.000044	0.000044	32.17	0.0001
Time on (μs)	2	0.000004	4.35	0.000004	0.000002	1.36	0.2930
Time off (μs)	2	0.000021	25.04	0.000021	0.000011	7.83	0.0067
Error	12	0.000016	19.18	0.000016	0.000001		
Total	17	0.000086	100.00		**R-sq: 80.82%**		
Analysis of variance for processing time							
Source	DF	Seq. SS	Contribution (%)	Adj. SS	Adj. MS	*F* value	*P* value
Ampere	1	235298	78.02	235298	235298	154.36	0.00000001
Time on (μs)	1	3536	1.17	3536	3536	2.32	0.14999385
Time off (μs)	1	41419	13.73	41419	41419	27.17	0.00013152
Error	14	21341	7.08	21341	1524		
Total	17	301594	100.00		**R-sq: 92.92%**		

Table 6: Regression equations for output results.

		Regression equations
Surface roughness (Ra, μm)	=	1.236 + 0.4794 ampere + 0.002653 Time on – 0.00709 Time off
Hole diameter (HD, mm)	=	12.4249 + 0.01883 ampere + 0.000273 Time on – 0.001531 Time off
Crater diameter (CD, mm)	=	46.35 + 13.492 ampere + 0.07028 Time on provide the DOI for "Zhao et al., 2016". 0.1222 Time off
Wear amount (WA, g)	=	0.4252–0.0204 ampere + 0.000291 Time on (μs) – 0.001512 Time off
Material removal rate (MRR, g/min)	=	0.00183 + 0.001566 ampere – 0.000002 Time on – 0.000066 Time off
Processing time (PT, min)	=	410.5–114.33 amper + 0.0858 Time on + 2.937 Time off

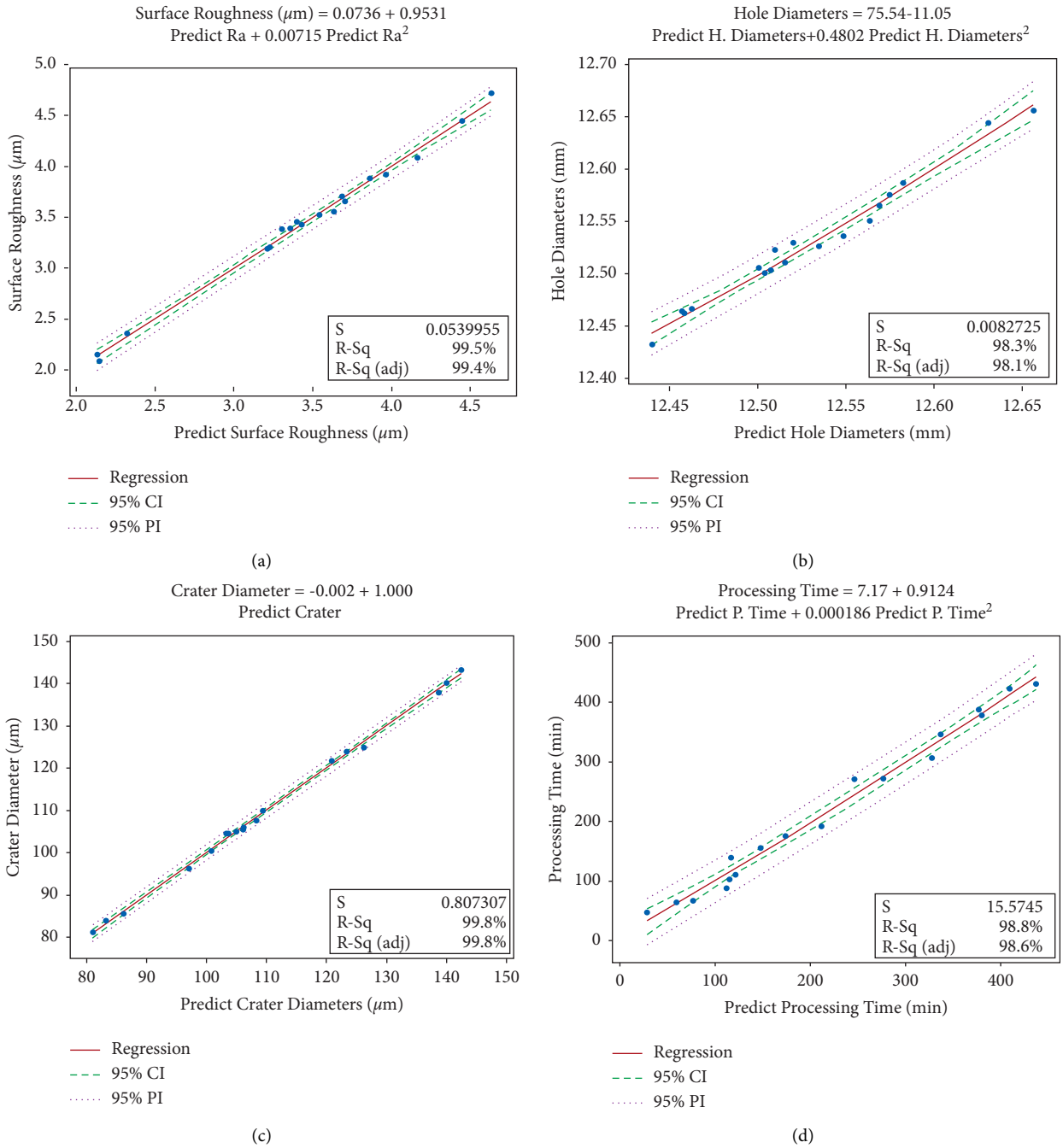

Figure 11: Continued.

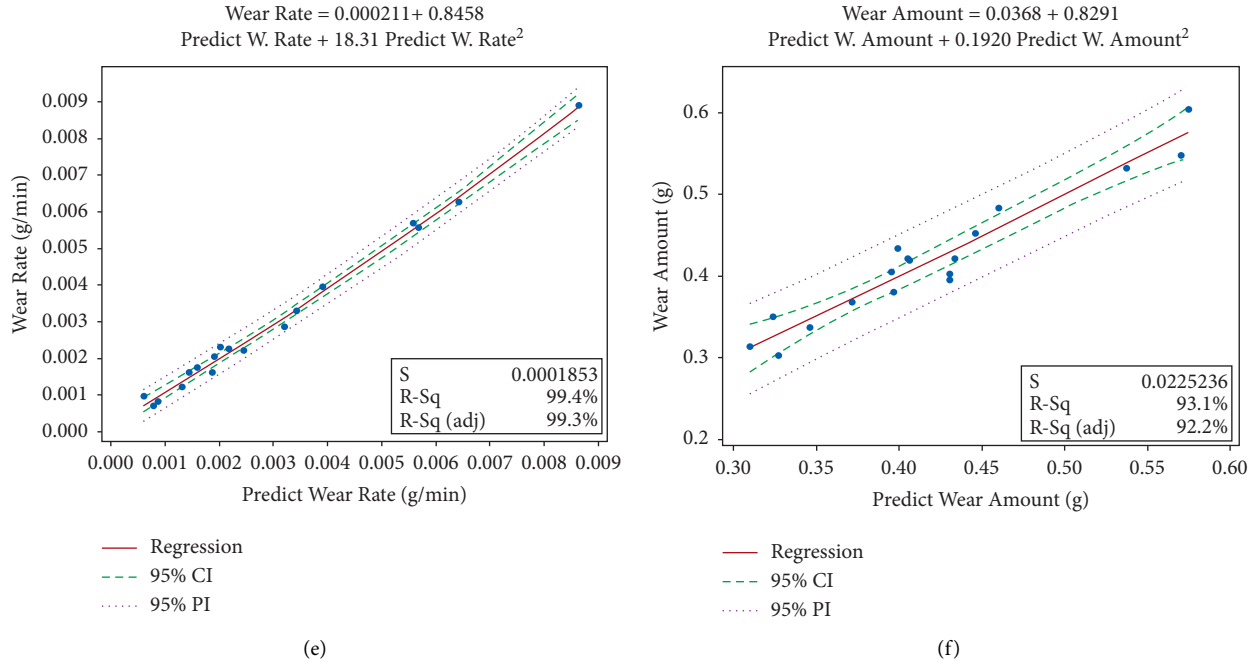

FIGURE 11: Graphs of estimated results and results obtained from experiments ((a) surface roughness, (b) hole diameter, (c) crater diameter, (d) wear amount, (e) wear rate, and (f) processing time).

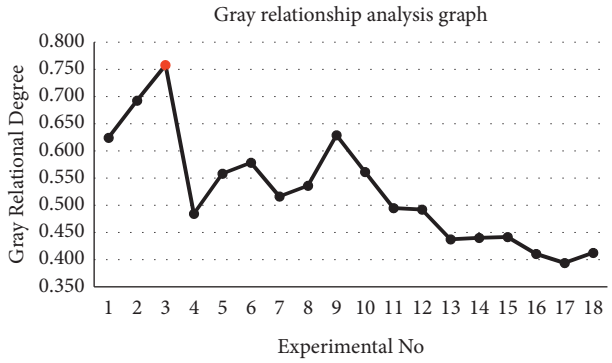

FIGURE 12: Gray correlation degree for lowest output parameters.

$$\varepsilon\left(x_0(k), x_j(k)\right) = \frac{\Delta_{\min} + \xi\Delta_{\max}}{\Delta_{oi}(k) + \xi\Delta_{\max}}, \tag{18}$$

$$\Delta_{oi}(k) = \left|x_0(k) - x_j(k)\right|, \tag{19}$$

$$\Delta_{\min} = \min_j \min_k \left|x_0(k) - x_j(k)\right|, \tag{20}$$

$$\Delta_{\max} = \max_j \max_k \left|x_0(k) - x_j(k)\right|. \tag{21}$$

ξ_ε is a coefficient between 0 and 1. J = 1, 2, . . ., m; $k = 1, 2, \ldots, n$. The function of ξ is to set the difference between Δ_{oi} and $\Delta_{\max}$. Studies show that the ξ value does not affect the ranking that will occur after the gray relational degree.

Step 5. The gray relational grade is calculated by the following equation:

$$\gamma(x_0, x_i) = \frac{1}{n}\sum_{k=1}^{n} \varepsilon\left(x_0(k), x_j(k)\right), \tag{22}$$

where $\gamma(x_0, x_i)$ is a measure of the geometric similarity between the x_i series and the x_0 reference series in a gray system. The magnitude of the gray relational degree indicates that there is a strong relationship between x_i and x_0. If the two sequences compared are the same, the gray relational degree is "1." The gray relational ranking tests the similarity of the two series. The gray relational degree can be found by multiplying the weight value indicating the significance of the criterion with the gray correlation coefficient of the

Table 7: Gray relational analysis and ranking.

Exp No.	Normalization						Coefficient matrix						
	Ra (μm)	HD (mm)	CD (μm)	MRR (g/min)	PT (min)	WA (g)	Ra (μm)	HD (mm)	CD (μm)	MRR (g/min)	PT (min)	WA (g)	Gray degree
1	0.894	0.848	0.929	0.182	0.379	0.396	0.825	0.767	0.875	0.379	0.446	0.453	0.624
2	0.976	0.866	0.955	0.063	0.781	0.396	0.954	0.789	0.918	0.348	0.695	0.453	0.693
3	1.000	1.000	1.000	0.030	0.888	0.218	1.000	1.000	1.000	0.340	0.817	0.390	0.758
4	0.502	0.408	0.621	0.109	0.587	0.439	0.501	0.458	0.569	0.360	0.548	0.471	0.484
5	0.574	0.565	0.691	0.012	0.979	0.116	0.540	0.535	0.618	0.336	0.960	0.361	0.558
6	0.579	0.652	0.756	0.000	1.000	0.000	0.543	0.589	0.672	0.333	1.000	0.333	0.579
7	0.444	0.362	0.574	0.162	0.582	0.812	0.473	0.439	0.540	0.374	0.545	0.727	0.516
8	0.488	0.540	0.600	0.126	0.676	0.759	0.494	0.521	0.555	0.364	0.607	0.675	0.536
9	0.507	0.598	0.623	0.110	0.864	1.000	0.504	0.554	0.570	0.360	0.786	1.000	0.629
10	0.401	0.683	0.534	1.000	0.000	0.386	0.455	0.612	0.518	1.000	0.333	0.449	0.561
11	0.454	0.696	0.608	0.607	0.052	0.261	0.478	0.622	0.561	0.560	0.345	0.403	0.495
12	0.479	0.857	0.615	0.262	0.164	0.040	0.489	0.778	0.565	0.404	0.374	0.342	0.492
13	0.302	0.310	0.295	0.680	0.042	0.310	0.417	0.420	0.415	0.610	0.343	0.420	0.437
14	0.317	0.583	0.310	0.398	0.144	0.340	0.423	0.545	0.420	0.454	0.369	0.431	0.440
15	0.386	0.673	0.345	0.189	0.282	0.158	0.449	0.604	0.433	0.381	0.411	0.373	0.442
16	0.000	0.000	0.000	0.592	0.104	0.601	0.333	0.333	0.333	0.551	0.358	0.556	0.411
17	0.103	0.054	0.048	0.314	0.238	0.498	0.358	0.346	0.344	0.422	0.396	0.499	0.394
18	0.240	0.470	0.085	0.193	0.337	0.330	0.397	0.486	0.353	0.382	0.430	0.427	0.413

Ra: surface roughness, HD: hole diameter, CD: crater diameter, WR: wear rate, PT: processing time, WA: wear amount.

criterion. The degree of gray relationship is calculated according to the following equation [34]:

$$\gamma(x_0, x_i) = \frac{1}{n}\sum_{k=1}^{n} \varepsilon\left(x_0(k), x_j(k), \left(w_i(k)\right)\right). \quad (23)$$

The gray relational degree graph (Figure 12) was formed according to the maximum and minimum values in the gray relational degree column in Table 7. After finding the coefficient matrices of the results from the experiments, the gray relational degree was calculated from the average of the values obtained [35, 36].

4. Conclusions

In this study, AISI D2 cold work tool steel chip removal was carried out on an EDM machine using different parameters. The results obtained were analyzed using both experimental and statistical methods and are summarized as follows.

The following was determined:

(i) In the experiments carried out with 2 amperes, the maximum processing time was 400 μs pulse time-on and 60 μs time-off, whereas the lowest processing time was 200 μs pulse time-on and 20 μs time-off

(ii) In the experiments carried out with 4 amperes, the minimum processing time was 200 μs pulse time-on and 20 μs time-off, whereas the maximum processing time was 600 μs pulse time-on and 60 μs time-off

(iii) The amount of material wear increased with decreasing time-off

(iv) The minimum material removal rate was 0.0007 g/min at 2 amperes, 400 μs pulse time-on, and 60 μs time-off

(v) The highest material removal rate was 0.0089 g/min at 4 amperes, 200 μs pulse time-on, and 60 μs time-off

(vi) The lowest surface roughness and crater diameter values occurred with current of 2 amperes, 200 μs pulse time-on, and 60 μs time-off, while the highest surface roughness and crater diameter values occurred with current of 4 amperes, 600 μs pulse time-on, and 20 μs time-off

(vii) Increased amperage and pulse duration affected the crater diameter, thereby affecting the material surface roughness negatively, while affecting the amount of material wear positively

(viii) With decreases in time-off, amperage, and pulse time-on, the hole diameter became larger than the diameter of the electrode

(ix) The most suitable parameters according to S/N ratios were $A_1B_1C_3$ for surface roughness, hole diameter, and crater diameter; $A_1B_3C_1$ for wear amount; $A_2B_1C_1$ for wear rate; and $A_1B_3C_3$ for processing time

(x) According to ANOVA results, the most effective parameters were amperage (49.34%) for surface roughness, time-on (59.38%) for hole diameter,

amperage (55.65%) for crater diameter, time-on (56.92%) for wear amount, amperage (51.42%) for material removal rate, and amperage for processing time (78.02%)

(xi) When the gray relational degree was calculated for the maximum and minimum values, the ideal factors for both occurred with the parameters applied in the third experiment ($A_1B_1C_3$)

Abbreviations

EDM: Electric discharge machining
RSM: Response surface methodology
MMR: Material removal rate
GA: Genetic algorithm
Ra: Surface roughness
W_i: Initial weight of workpiece (before machining)
W_f: Final weight of workpiece (after machining)
t: Period of trial
SEM: Scanning electron microscope
S/N: Signal-to-noise
HD: Hole diameter
CD: Crater diameter
WA: Wear amount
PT: Processing time
CI: Confidence interval
PI: Predicted internally
F: F ratio at 95% (at F table)
α: Significance level
fe: Degrees of freedom of error
Ve: Error variance
r: Number of replications for confirmation experiment
n_{eff}: Effective number of replications
N: Total number of experiments
T_{dof}: Total main factor degrees of freedom.

Data Availability

The data used to support the findings of this study are available from the corresponding author or from within article, upon request.

Conflicts of Interest

The authors declare that they have no conflicts of interest.

References

[1] F. Kara, "Optimization of surface roughness in finish milling of AISI P20+s plastic-mold steel," *Materials and Technology*, vol. 52, no. 2, pp. 195–200, 2018.

[2] M. Süzgünol and Y. Kayır, "Machinability of DIN 1.2311 and 1.2738 mold steels," in *Proceedings of the 3rd National Machining Symposium*, pp. 132–142, Singapore, February 2012.

[3] J. Lee, "Modern manufacturing," *Mechanical Engineering Handbook*, CRC pres, Boca Raton, LLC, 1999.

[4] O. Gülcan, "Electro-erosion processing in pure water," *Engineer and Machinery*, vol. 55, no. 648, pp. 28–36, 2013.

[5] K. H. Ho and TS. Newman, "State of the art electrical discharge machining," *International Journal of Machine Tools and Manufacture*, vol. 37, no. 11, pp. 1287–1300, 2003.

[6] M. N. Abbas, G. D. Solomon, and F. M. Bahari, "A review on current research trends in electrical discharge machining (EDM)," *Journal of Machine Tools & Manufacture*, vol. 47, no. 7-8, pp. 1214–1228, 2007.

[7] N. Masmiati, A. A. D. Sarhan, and D. Sarhan, "Optimizing cutting parameters in inclined end milling for minimum surface residual stress - taguchi approach," *Measurement*, vol. 60, pp. 267–275, 2015.

[8] R. Z. Lazic, *Design of Experiments in Chemical Engineering: A Practical Guide*, pp. 157–165, Wiley VCH, Weinheim, 2004.

[9] W. H. Yang and Y. S. Tarng, "Design optimization of cutting parameters for turning operations based on the taguchi method," *Journal of Materials Processing Technology*, vol. 84, no. 1-3, pp. 122–129, 1998.

[10] C. Hamzaçebi and F. Kutay, "Taguchi method: an application," *Technology*, vol. 3, no. 4, pp. 7–17, 2003.

[11] K. Nagaraja, A. M. Herbert, D. Shetyy, R. Shetyy, and B. Shivamurty, "Effect of process parameters on delamination, thrust force and torque in drilling of carbon fiber epoxy composite," *Research Journal of Recent Sciences*, vol. 2, no. 8, pp. 47–51, 2013.

[12] E. Nas, K. Argun, and E. Zurnacı, "Experimental and statistical investigation of effects of machining parameters on surface roughness at machining with graphite and copper electrode in electro discharge machining of AISI 1.2738 steel," *Duzce University Journal of Science and Technology*, vol. 6, pp. 1082–1093, 2018.

[13] G. Taguchi, S. Chowdhury, and Y. Wu, *Taguchi's Quality Engineering Handbook*, John Wiley & Sons, New Jersey, NJ, USA, 2005.

[14] E. Nas and H. Gökkaya, "Experimental and statistical study on machinability of the composite materials with metal matrix Al/B4C/Graphite," *Metallurgical and Materials Transactions A*, vol. 48, no. 10, pp. 5059–5067, 2017.

[15] R. Matin, R. M. Shabgard, and R. Barzegar, "Effect of electrode shape configuration on tool steel (DIN1.2379) in electrical discharge machining (EDM)," in *Proceedings of the National Conference on Economics, Management and Accounting*, pp. 1–8, USA, June 2013.

[16] K. Gov, "The Effects of the dielectric liquid temperature on the hole geometries drilled by electro erosion," *International Journal of Advanced Manufacturing Technology*, vol. 92, no. 1-4, pp. 1255–1262, 2017.

[17] K. Gov, "Experimental investigation of the effects of electrodes on edm hole drilling process," *Journal of Polytechnic*, vol. 20, no. 2, pp. 377–382, 2017.

[18] J. Anitha, R. Das, and M. K. Pradhan, "Optimization of surface roughness in EDM for D2 steel by RSM-GA approach," *Universal Journal of Mechanical Engineering*, vol. 2, no. 6, pp. 205–210, 2014.

[19] A. Kalyon, "Experimental investigation of the machinability of AISI D2 cold work tool steel with electro discharge technique," *Journal of Applied Sciences of Mehmet Akif Ersoy University*, vol. 3, no. 1, pp. 75–86, 2019.

[20] D. A. Çuhadaroğlu and E. Kara, "Graphite: an overview," *SDU Journal Of Technical Sciences*, vol. 8, no. 1, pp. 14–33, 2018.

[21] A. Sağlam Metal: https://www.saglammetal.com/tr/urun-detay/takim-celikleri/soguk-is-takim-celikleri/12379-cppu-celik (accessed October 10, 2019.

[22] A. Uğur, E. Nas, and H. Gökkaya, "Investigation of the machinability of SiC reinforced MMC materials produced by

molten metal stirring and conventional casting technique in die-sinking electrical discharge machine," *International Journal of Mechanical Sciences*, vol. 186, Article ID 105875, 2020.

[23] V. Yılmaz, M. Özdemir, and H. Dilipak, "AISI 1040 çeliğinin elektro erozyon ile işleme yöntemiyle delinmesinde işleme parametrelerinin temel performans çıktıları üzerindeki etkilerinin incelenmesi," *Gazi Üniversitesi Fen Bilimleri Dergisi PART C: Tasarım Ve Teknoloji*, vol. 3, no. 1, pp. 417–426, 2015.

[24] P. H. Nguyen, L. T. Banh, V. D. Bui, and D. T. Hoang, "Multi-response optimization of process parameters for powder mixed electro-discharge machining according to the surface roughness and surface micro-hardness using taguchi-TOPSIS," *International Journal of Data and Network Science*, vol. 2, no. 4, pp. 109–119, 2018.

[25] S. Shankar, S. Maheshwaria, and P. C. Pandey, "Some investigations into the electric discharge machining of hardened tool steel using different electrode materials," *Journal of Materials Processing Technology*, vol. 149, pp. 272–277, 2004.

[26] S. L. Chen, B. H. Yan, and F. Y. Huang, "Influence of kerosene and distilled water as dielectrics on the electric discharge machining characteristics of Ti-6Al-4V," *Journal of Materials Processing Technology*, vol. 87, no. 1-3, pp. 107–111, 1999.

[27] M. Günay and E. Yücel, "Application of taguchi method for determining optimum surface roughness in turning of high-alloy white cast iron," *Measurement*, vol. 46, no. 2, pp. 913–919, 2013.

[28] E. Nas and S. Akıncıoğlu, "Optimization of cryogenic treated nickel-based superalloy in terms of electro erosion processing performance," *Academic Platform Journal of Engineering and Science*, vol. 7, no. 1, pp. 115–126, 2019.

[29] G. Sur and Ö. Erkan, "Cutting tool geometry in the drilling of cfrp composite plates and taguchi optimization of the cutting parameters affecting delamination," *Sigma Journal of Engineering and Natural Sciences*, vol. 36, no. 3, pp. 619–628, 2018.

[30] M. Ay and A. Turhan, "Investigation of the effect of cutting parameters on the geometric tolerances and surface roughness in turning operation," *Electronic Journal of Machine Technologies*, vol. 7, no. 3, pp. 55–67, 2010.

[31] S. Akıncıoğlu, H. Gökkaya, and İ. Uygur, "The Effects of cryogenic-treated carbide tools on tool wear and surface roughness of turning of hastelloy C22 based on taguchi method," *International Journal of Advanced Manufacturing Technology*, vol. 82, no. 1-4, pp. 303–314, 2016.

[32] E. Nas and B. Öztürk, "Optimization of surface roughness via the Taguchi method and investigation of energy consumption when milling spheroidal graphite cast iron materials," *Materials Testing*, vol. 60, no. 5, pp. 519–525, 2018.

[33] N. Tosun, "Determination of optimum parameters for multi-performance characteristics in drilling by using gray relational analysis," *International Journal of Advanced Manufacturing Technology*, vol. 28, no. 5-6, pp. 450–455, 2006.

[34] E. Yılmaz and F. güngör, "Determination of optimum tool holder with different hardness according to gray relational analysis method," in *Proceedings of the 2nd National Design Manufacturing and Analysis Congress*, pp. 1–5, Balıkesir, Turkey, 2010.

[35] R. B. Azhiri, A. S. Bideskan, F. Javidpour, and R. M. Tekiyeh, "Study on material removal rate, surface quality, and residual stress of AISI D2 tool steel in electrical discharge machining in presence of ultrasonic vibration effect," *International Journal of Advanced Manufacturing Technology*, vol. 101, no. 9-12, pp. 2849–2860, 2019.

[36] M. Patel Gowdru Chandrashekarappa, S. Kumar, J. Jagadish, D. Y. Pimenov, and K. Giasin, "Experimental analysis and optimization of EDM parameters on HcHcr steel in context with different electrodes and dielectric fluids using hybrid taguchi-based PCA-utility and CRITIC-utility approaches," *Metals*, vol. 11, no. 3, p. 419, 2021.